Evidence of an Alternative Mechanism for the Reductive Coupling of Isonitriles by Electrophilic 1-Sila-3-zirconacyclobutane Complexes. Structural Characterization of the Bicyclic Enediamido Complexes $Cp_2Zr(N(CMe_3)C(CH_2SiMe_2CH_2)=CN(R))$, Where R = *tert*-Butyl and 2,6-Xylyl

Frederic J. Berg and Jeffrey L. Petersen*

Department of Chemistry, West Virginia University, Morgantown, West Virginia 26506-6045

Received October 23, 1990

The reductive coupling of 2 equiv of CN-*t*-Bu by $Cp_2Zr(CH_2SiMe_2CH_2)$ proceeds sequentially with the formation of the η^2-iminoacyl complex $Cp_2Zr(N(CMe_3)CCH_2SiMe_2CH_2)$ (1) and the η^2-iminoacyl imine complex $Cp_2Zr(N(CMe_3)C\text{-}C(=NCMe_3)CH_2SiMe_2CH_2)$ (2), which upon heating to 120 °C rearranges to the bicyclic enediamido complex $Cp_2Zr(N(CMe_3)C(CH_2SiMe_2CH_2)=CN(CMe_3))$ (3). Labeling experiments using a ^{13}C-enriched sample of 1 indicate that the insertion of the second equivalent of CN-*t*-Bu proceeds with nucleophilic displacement of the original η^2-iminoacyl group and does *not* involve the breaking of the C(η^2-iminoacyl)–C(methylene) bond of 1. Treatment of 1 with 2,6-xylyl isocyanide proceeds directly at 25 °C to yield the bicyclic enediamidate complex $Cp_2Zr(N(CMe_3)C(CH_2SiMe_2CH_2)=CN(xy))$ (5). From kinetic measurements within the temperature range 80–120 °C, the activation parameters for the first-order conversion of 2 to 3 are $\Delta H^{\ddagger}$ = 25.6 (5) kcal/mol and $\Delta S^{\ddagger}$ = −5.0 (9) eu. The corresponding reaction of 2 with 2,6-xylyl isocyanide affords only 3 upon heating, thus ruling out the possibility of isocyanide deinsertion being important during this intramolecular rearrangement. Complexes 3 and 5 were characterized by infrared and electronic spectroscopy, by variable-temperature NMR measurements, and by elemental analyses. Their molecular structures were determined by X-ray crystallographic methods. Crystal data for 3 at 22 °C: monoclinic space group $P2_1$ with a = 9.218 (2) Å, b = 9.186 (2) Å, c = 14.923 (2) Å, β = 101.95 (2)°, and Z = 2. For 5 at 22 °C: monoclinic $P2_1/c$ with a = 15.775 (3) Å, b = 8.169 (2) Å, c = 20.924 (4) Å, β = 97.36 (1)°, and Z = 4. The collective outcome of these experiments is consistent with an alternative mechanism being operative for the reductive coupling of isocyanides by a 1-sila-3-zirconacyclobutane complex.

Introduction

The transition-metal-mediated reductive coupling of C_1-fragments represents a potentially important carbon–carbon-bond-forming reaction in Fischer–Tropsch chemistry.[1] This type of reaction has been observed by several research groups during their investigations of the migratory insertion of CO and CNR into high-valent metal–alkyl[2–5] and –hydride[6–10] bonds.[11] The formation of the observed mono- and dinuclear enediolato or enediamido complexes was rationalized initially by invoking an intramolecular or intermolecular coupling of two η^2-acyl, η^2-formyl, or η^2-iminoacyl groups. The first direct support for this coupling mechanism was provided by Rothwell and co-workers[5] from their studies of a series of bis(η^2-iminoacyl) complexes, $M(OAr)_2(\eta^2\text{-}R'CNR)_2$ (M = Ti, Zr, Hf), which transform on thermolysis to the corresponding enediamidate complexes, $M(OAr)_2[R'NC(R)=C(R)NR']$. Although the reductive CO coupling reactions originally reported by Bercaw and co-workers for $Cp^*_2ZrMe_2$[2] and later described by Marks and co-workers for $Cp^*_2MR_2$ (M = Th, U; R = Me, CH_2SiMe_3)[4] were thought to involve the participation of an incipient bis(oxycarbene) species, recent theoretical[12,13] and experimental[13,14] results indicate an alternative pathway leading to the enediolate product is probably operative. Roddick and Bercaw,[14] on the basis of their reactivity studies of η^2-aldehyde adducts of permethylzirconocene and permethylhafnocene, propose that the key steps in the reductive coupling of CO by $Cp^*_2ZrMe_2$ are methyl migration to the electrophilic carbon of the initial η^2-acyl ligand, CO insertion into the Zr–C

(1) *Catalytic Activation of Carbon Monoxide*; Ford, P. C., Ed.; ACS Symposium Series 152; American Chemical Society: Washington, DC, 1981.
(2) Manriquez, J. M.; McAlister, D. R.; Sanner, R. D.; Bercaw, J. E. *J. Am. Chem. Soc.* **1978**, *100*, 2716.
(3) Hofmann, P.; Frede, M.; Stauffert, P.; Lasser, W.; Thewalt, U. *Angew. Chem., Int. Ed. Engl.* **1985**, *24*, 712.
(4) (a) Manriquez, J. M.; Fagan, P. J.; Marks, T. J.; Day, C. S.; Day, V. W. *J. Am. Chem. Soc.* **1978**, *100*, 7112. (b) Fagan, P. J.; Manriquez, J. M.; Marks, T. J.; Day, V. W.; Vollmer, S. H.; Day, C. S. *J. Am. Chem. Soc.* **1980**, *102*, 5396. (c) Moloy, K. G.; Fajan, P. J.; Manriquez, J. M.; Marks, T. J. *J. Am. Chem. Soc.* **1986**, *108*, 56.
(5) (a) McMullen, A. K.; Rothwell, I. P.; Huffman, J. C. *J. Am. Chem. Soc.* **1985**, *107*, 1072. (b) Latesky, S. L.; McMullen, A. K.; Niccolai, G. P.; Rothwell, I. P.; Huffman, J. C. *Organometallics* **1985**, *4*, 1896. (c) Chamberlain, L. R.; Durfee, L. D.; Fanwick, P. E.; Kobriger, L. M.; Latesky, S. L.; McMullen, A. K.; Steffey, B. D.; Rothwell, I. P.; Folting, K.; Huffman, J. C. *J. Am. Chem. Soc.* **1987**, *109*, 6068. (d) Durfee, L. D.; McMullen, A. K.; Rothwell, I. P. *J. Am. Chem. Soc.* **1988**, *110*, 1463.
(6) Wolczanski, P. T.; Bercaw, J. E. *Acc. Chem. Res.* **1980**, *13*, 121.
(7) Evans, W. J.; Grate, J. W.; Doedens, R. J. *J. Am. Chem. Soc.* **1985**, *107*, 1671.
(8) Bocarsly, J. R.; Floriani, C.; Chiesa-Villa, A.; Guastini, C. *Organometallics* **1986**, *5*, 2380.
(9) Moloy, K. G.; Marks, T. J. *J. Am. Chem. Soc.* **1984**, *106*, 7051 and references cited therein.
(10) Fajan, P. J.; Manriquez, J. M.; Vollmer, S. H.; Day, C. S.; Day, V. W.; Marks, T. J. *J. Am. Chem. Soc.* **1981**, *103*, 2206.
(11) Notable examples of isonitrile coupling reactions by low-valent organometallic alkyl complexes include: (a) Yamamoto, Y.; Yamazaki, H. *Inorg. Chem.* **1977**, *16*, 3182 and references cited therein. (b) Motz, P. J.; Alexander, J. J.; Ho, D. M. *Organometallics* **1989**, *8*, 2589 and references cited therein.
(12) Tatsumi, K.; Nakamura, A.; Hofmann, P.; Hoffmann, R.; Moloy, K. G.; Marks, T. J. *J. Am. Chem. Soc.* **1986**, *108*, 4467.
(13) Hofmann, P.; Stauffert, P.; Frede, M.; Tatsumi, K. *Chem. Ber.* **1989**, *122*, 1559.
(14) Roddick, D. M.; Bercaw, J. E. *Chem. Ber.* **1989**, *122*, 1579.

0276-7333/91/2310-1599$02.50/0

bond of an intermediate η^2-acetone adduct, and a 1,2-methyl shift to a η^2-acyl carbon atom. This intramolecular pathway is consistent with cross-over experiments,[12,13] which confirm that enediolate formation occurs at a single metal center.

Recent investigations in our laboratory have shown that the reactions of CO[15] and CNMe[16] with $Cp^*_2Zr(CH_2SiMe_2CH_2)$ proceed under orbital control with the facile formation of related bicyclic enediolate and enediamidate complexes, $Cp^*_2Zr(OC(CH_2SiMe_2CH_2)=CO)$ and $Cp^*_2Zr(N(Me)C(CH_2SiMe_2CH_2)=CN(Me))$, respectively. Subsequent studies[16] of the reaction of *tert*-butyl isocyanide with $Cp_2Zr(CH_2SiMe_2CH_2)$ have led to the isolation of two "carbenium-like" η^2-iminoacyl intermediates, $Cp_2Zr(N(CMe_3)CCH_2SiMe_2CH_2)$ (1) and $Cp_2Zr(N(CMe_3)C{-}C(=NCMe_3)CH_2SiMe_2CH_2)$ (2), which directly participate in the coupling of two CN-*t*-Bu molecules. Mechanistic information about this reductive coupling process has been obtained by reacting the η^2-iminoacyl complex, 1, and the η^2-iminoacyl imine complex, 2, with 2,6-xylyl isocyanide and by reacting a ^{13}C-enriched sample of 1 with CN-*t*-Bu. The outcome of these experiments and our X-ray structural analyses of the bicyclic enediamidate complexes $Cp_2Zr(N(CMe_3)C(CH_2SiMe_2CH_2)=CN(R))$, where R = CMe_3 and 2,6-xylyl, are described herein. The collective results indicate that the coupling reactions displayed by these 1-sila-3-zirconacyclobutane complexes involve a different sequence of reaction steps and have led us to propose an alternative reaction mechanism.

Experimental Section

General Considerations. All reactions and manipulations were performed by using glovebox and high-vacuum techniques. Inert gases were prepurified by passage through columns containing activated BTS catalyst and 4A molecular sieves. Glassware was flame-dried under vacuum prior to use. Solvents were purified by standard procedures and then stored in storage flasks containing $[Cp_2Ti(\mu\text{-}Cl)_2]_2Zn$.[17] Benzene-$d_6$, chloroform-$d_1$, and toluene-$d_8$ were vacuum distilled from 4A molecular sieves. *tert*-Butyl isocyanide (Aldrich) was dried over activated molecular sieves and distilled before use. A ca. 20% ^{13}C-enriched sample of *tert*-butyl isocyanide was prepared by the procedure described below. $H^{13}COOH$ (99%, Cambridge Isotrope Laboratories), HCOOH (Aldrich), *tert*-butylamine (Aldrich), 1,3-dicyclohexylcarbodiimide (Aldrich), $POCl_3$ (Aldrich), and 2,6-xylyl isocyanide (Fluka) were used as received. $Cp_2Zr(CH_2SiMe_2CH_2)$[18] and $Cp_2Zr(N(CMe_3)CCH_2SiMe_2CH_2)$[16] were prepared by published procedures. The quantitative addition of volatile isocyanides to a reaction was done by using a calibrated gas bulb equipped with high-vacuum Teflon stopcocks. Elemental analyses were performed by Oneida Research Services of Whitesboro, NY (ORS).

^1H and ^{13}C NMR spectra were measured on a JEOL GX-270 FT-NMR spectrometer operating in the FT mode at 270 (^1H) and 67.5 MHz (^{13}C). The ^1H chemical shifts are referenced to the residual proton peak of benzene-d_6 (δ 7.15) or chloroform-d_1 (δ 7.24) or to the methyl proton peak of toluene-d_8 (δ 2.09); the ^{13}C resonances are referenced to the central carbon peak of benzene-d_6 (δ 128.0) or chloroform-d_1 (δ 77.0) or to the methyl carbon peak of toluene-d_8 (δ 20.4). IR spectra were measured on a Perkin-Elmer 1310 infrared spectrometer using KBr disks and calibrated against polystyrene. Electronic spectra were recorded on a Hewlett-Packard 8452A diode array spectrometer using a 1.00-cm quartz cell equipped with a Teflon stopcock.

Kinetic Measurements. The thermal rearrangement of 2 to $Cp_2Zr(N(CMe_3)C(CH_2SiMe_2CH_2)=CN(CMe_3))$ was followed for over 3 half-lives by monitoring the loss of the intensity of its cyclopentadienyl ring proton resonance in toluene-d_8 solutions (0.106 mM) in a sealed NMR tube. Ferrocene was used as the internal integration standard. Reaction temperatures were maintained to ±0.1 °C with a Neslab Exacal constant-temperature bath. The NMR tubes were submerged totally in the oil bath. To check the reliability of our kinetic measurements, two different procedures were considered initially. One set of experiments employed five NMR sample tubes, which were submerged simultaneously and then removed individually at different predetermined times. The alternative approach used only one NMR sample tube, removing it periodically to measure the NMR spectrum and then returning it to the oil bath. Each time an NMR tube was removed from the oil bath, it was cooled immediately in an ice–water slush to quench the rearrangement reaction. Because the rate constants obtained by these two procedures for 2 → 3 at 110 °C agreed within 4%, the latter procedure was employed for the remaining kinetic experiments. Repeated NMR measurements employing a pulse delay of 20 s demonstrated that the integrated intensities were reproducible to within ±6%. Each spectrum was recorded three times, and the average integrated intensity was used in the determination of k at each temperature. The values of the activation parameters, $\Delta H^\ddagger$ and $\Delta S^\ddagger$, were calculated from a plot of $-\ln(k/T)$ vs $1/T$, assuming a value of 1 for the transmission coefficient in the Eyring equation, $\Delta G^\ddagger(T) = RT \ln(\kappa k_B T/kh)$.

Preparation of 20% ^{13}C-Enriched *tert*-Butyl Isocyanide. To a 250-mL, three-neck flask equipped with a dropping funnel and N_2 inlet and outlet adapters were added 55 mL of dry CH_2Cl_2, 15 mL (0.143 mol) of *tert*-butylamine, and 29.7 g (0.144 mol) of dicyclohexylcarbodiimide under a N_2 flush. To the addition funnel was added 1.0 mL of 99% ^{13}C-enriched formic acid and 4.0 mL of unlabeled formic acid (total of 0.126 mol). The reaction mixture was cooled in an ice bath, and the formic acid was added dropwise with rapid stirring over a 30-min period. Upon completion of the addition, the reaction was stirred at room temperature for another 4 h. After removal of the solvent, the product was isolated by distillation using a Vigreux column and its purity was checked by ^1H NMR spectroscopy (10.57 g, 79% yield, bp 88–90 °C at 20 mTorr). Subsequent dehydration of the *tert*-butylformamide with $POCl_3$ following a literature procedure[19] gave the desired ^{13}C-enriched *tert*-butyl isocyanide, which was purified by using a microscale spinning band distillation column (3.79 g, 46% yield).

Preparation of $Cp_2Zr(N(CMe_3)C(CH_2SiMe_2CH_2)=CN(CMe_3))$ (3). A freshly sublimed sample of $Cp_2Zr(CH_2SiMe_2CH_2)$ (0.485 g, 1.58 mmol) was added to a 100-mL pear-shaped flask attached via a solv-seal joint to a calibrated gas bulb. Toluene was condensed onto the solid, and the gas bulb was charged with 2 equiv of CN-*t*-Bu. After the flask was cooled to below −70 °C, the CN-*t*-Bu was admitted by opening the Teflon stopcock. The reaction mixture was stirred for 5 days at room temperature and then heated for 24 h at 120 °C. The yellow product was washed twice with hexamethyldisiloxane, dried in vacuo overnight, and recrystallized with pentane (90% isolated yield). Crystals suitable for an X-ray structural analysis were obtained by slow removal of pentane from a saturated solution.

IR (KBr): 1610 (C=C stretch, weak) cm^{-1}. ^1H NMR spectrum in benzene-d_6 (mult, $^2J_{H\text{-}H}$ in Hz): δ 6.06, 5.37 (C_5H_5, s), 2.01, 1.20 (CH_aH_b, d, 16.9), 1.39 ($NCCH_3$, s), 0.21, 0.16 ($SiCH_3$, s). Gated nondecoupled ^{13}C NMR spectrum in benzene-d_6 (mult, $^1J_{^{13}C\text{-}H}$ in Hz): δ 122.3 (*N*C=, s), 108.2, 103.1 (C_5H_5, d, 170), 58.6 (*N*CCH_3, s), 34.4 (NC*C*H_3, q, 125), 22.4 (CH_2, t, 123), −2.21, −2.84 ($SiCH_3$, q, 119, 118). Anal. Calcd for $C_{24}H_{38}N_2SiZr$: C, 60.83; H, 8.08; N, 5.91. Found: C, 60.11; H, 8.08; N, 5.40. λ_{max} = 352 nm, ϵ_{max} = 5.12 × 10^3 L mol^{-1} cm^{-1}.

(15) Petersen, J. L.; Egan, J. W., Jr. *Organometallics* **1987**, *6*, 2007.
(16) Berg, F. J.; Petersen, J. L. *Organometallics* **1989**, *8*, 2461.
(17) Sekutowski, D. G.; Stucky, G. D. *Inorg. Chem.* **1975**, *14*, 2192.
(18) Tikkanen, W.; Liu, J. Z.; Egan, J. W., Jr.; Petersen, J. L. *Organometallics* **1984**, *3*, 825.
(19) Casanova, J., Jr.; Werner, N. D.; Schuster, R. E. *J. Org. Chem.* **1966**, *31*, 3473.

Preparation of $Cp_2Zr(N(CMe_3)C(CH_2SiMe_2CH_2)=CN(xy))$ (5). A 0.612-g (1.57 mmol) sample of $Cp_2Zr(N(CMe_3)CCH_2SiMe_2CH_2)$ and a 0.212-g (1.62 mmol) sample of 2,6-xylyl isocyanide were added to separate 100-mL solv-seal flasks that were then connected to a pressure-equalizing swivel frit assembly. After 30 mL of toluene was added to each flask, the solution containing 2,6-xylyl isocyanide was added in small increments over a period of 3 days. The red oil remaining after removal of the solvent was washed twice with hexamethyldisiloxane. The light orange residue was dried overnight and recrystallized with pentane (32% isolated yield). Crystals for the X-ray structure determination were obtained by slow removal of pentane from a saturated solution.

IR (KBr): 1585 (C=C stretch, weak) cm^{-1}. ^1H NMR spectrum in chloroform-d_1 (mult, $^2J_{H-H}$ in Hz): δ 6.9–7.1 (meta and para C–H, m), 5.79, 5.69 (C_5H_5, s), 2.44, 1.60 (C–CH_3, s), 2.09, 1.55 (CH_aH_b, d, 17.0), 1.39 ($NCCH_3$, s), 1.29, 1.06 (CH_cH_d, d, 17.8), 0.26, 0.17 ($SiCH_3$, s). Gated nondecoupled ^{13}C NMR spectrum in chloroform-d_1 (mult, $^1J_{^{13}C-H}$ in Hz): δ 151.2 (CNC, s), 133.9, 131.6 (CCH_3, s), 128.0, 127.9, 122.9 (meta and para carbons, d, 156, 156, 159), 123.9, 122.5 (NC=, s), 109.0, 104.5 (C_5H_5, d, 172, 170), 57.5 ($NCCH_3$, s), 33.5 ($NCCH_3$, q, 125), 22.1 (CH_aH_b, t, 125), 21.2, 17.4 (CCH_3, q, 122), 16.9 (CH_cH_d, t, 125), –1.20, –1.26 ($SiCH_3$, q, 120). Anal. Calcd for $C_{28}H_{38}N_2SiZr$: C, 64.44; H, 7.34; N, 5.37. Found: C, 64.52; H, 7.25; N, 5.03. λ_{max} = 366 nm, $\epsilon_{max} = 4.18 \times 10^3$ L mol^{-1} cm^{-1}.

X-ray Data Collection. The X-ray structural analyses of $Cp_2Zr(N(CMe_3)C(CH_2SiMe_2CH_2)=CN(R))$, where R = *tert*-butyl (3) and 2,6-xylyl (5), were performed by following the same general procedures.[20] Each crystal was sealed in a glass capillary tube under a prepurified N_2 atmosphere and then optically aligned on a Picker goniostat under computer control by a Krisel Control diffractometer automation system. Following an initial evaluation of low-angle reflections, the orientation angles of 20 higher order reflections were optimized by an automatic peak-centering routine and then least-squares fit to provide the corresponding refined lattice parameters (Table I) and the orientation matrix.

Intensity data ($\pm h,k,l$) were measured with Zr-filtered Mo Kα X-ray radiation with a takeoff angle of 2°. Peak scans (θ–2θ mode) were made with a fixed scan rate and a variable scan width. The integrated intensity, I, and its standard deviation, $\sigma_c(I)$, for each measured reflection were calculated from the equations $I = w(S/t_s - B/t_b)$ and $\sigma_c(I) = w(S/t_s^2 + B/t_b^2)^{1/2}$, where S is the total scan count measured in time t_s and B is the combined background count in t_b. The standard deviation of the square of each structure factor, $F_o^2 = I/Lp$, was calculated from $\sigma_c(F_o^2) = [\sigma_c(F_o^2)^2 + (pF_o^2)^2]^{1/2}$. Duplicate reflections were averaged. Further crystallographic information is summarized in Table I.

Structural Solution and Refinement. Initial coordinates for the Zr atom in 3 were determined by an interpretation of the Harker vectors provided by an unsharpened Patterson map, whereas the position of the Zr atom in 5 was interpolated from an E map calculated on the basis of phases determined by MULTAN78.[21] Approximate coordinates for the remaining non-hydrogen atoms in each compound were obtained from subsequent Fourier summations and were refined with anisotropic thermal parameters. All of the hydrogen atoms were located by using difference Fourier calculations which employed only low-angle data with $(\sin\theta)/\lambda < 0.40$ Å^{-1}. Full-matrix refinement (based on F_o^2)[22-26] of the positional and anisotropic thermal parameters for the 28 non-hydrogen atoms with fixed isotropic contributions for the 38 hydrogen atoms of 3 led to final discrepancy indices of $R(F_o) = 0.055$, $R(F_o^2) = 0.073$, and $R_w(F_o^2) = 0.093$ with $\sigma_1 = 1.71$ for the 1593 reflections with $F_o^2 > \sigma(F_o^2)$. The values of these indices are slightly higher for the other enantiomorph, for which the corresponding coordinates are determined by reversing the signs of all of the atomic fractional coordinates. The corresponding anisotropic refinement of the 32 non-hydrogen atoms with isotropic temperature factors for the 38 hydrogen atoms of 5 converged with final discrepancy indices of $R(F_o) = 0.051$, $R(F_o^2) = 0.051$, and $R_w(F_o^2) = 0.084$ with $\sigma_1 = 1.64$ for the 4009 reflections with $F_o^2 > \sigma(F_o^2)$. A final difference Fourier summation was calculated in each case and did not reveal any significant regions of residual electron density.

The positional parameters for the refined atoms are provided in Tables II and III for 3 and 5, respectively. Selected interatomic distances and bond angles and their esd's for the non-hydrogen atoms are given in Table IV for 3 and Table V for 5. Tables of thermal parameters, the equations of pertinent least-squares planes and their dihedral angles, and tables of observed and calculated structure factors are available as supplementary material.

Table I. Data for X-ray Diffraction Analysis of $Cp_2Zr(N(CMe_3)C(CH_2SiMe_2CH_2)=CN(CMe_3))$ (3) and $Cp_2Zr(N(CMe_3)C(CH_2SiMe_2CH_2)=CN(xy))$ (5)

	3	5
A. Crystal Data		
cryst syst	monoclinic	monoclinic
space group	$P2_1$ (C_2^2, No. 4)	$P2_1/c$ (C_{2h}^5, No. 14)
a, Å	9.218 (2)	15.775 (3)
b, Å	9.186 (2)	8.169 (2)
c, Å	14.923 (2)	20.924 (4)
β, deg	101.95 (2)	97.36 (1)
V, Å^3	1236.2 (5)	2674.3 (9)
fw	473.89	521.93
d(calcd), g/cm^3	1.273	1.296
Z	2	4
μ, cm^{-1}	4.94	4.67
B. Data Collection and Analysis Summary		
cryst dimens, mm	0.275 × 0.175 × 0.100	0.500 × 0.300 × 0.350
no. of reflns sampled	$\pm h,k,l$ ($5° \le 2\theta \le 45°$)	$\pm h,k,l$ ($5° \le 2\theta \le 50°$)
2θ range for centered reflns, deg	24–31	30–36
scan rate, deg/min	2	2
scan width, deg	1.1 + 0.9 tan θ	1.1 + 0.8 tan θ
no. of std reflns	3	3
% cryst decay	none	4
total no. of measd reflns	1811	4942
no. of unique data used	1738	4744
agreement between equivalent data		
$R_{av}(F_o)$	0.041	0.030
$R_{av}(F_o)^2$	0.055	0.025
transm coeff	1.0	1.0
p	0.03	0.03
discrepancy indices ($F_o^2 > \sigma(F_o^2)$)		
$R(F_o)$	0.055	0.051
$R(F_o^2)$	0.073	0.051
$R_w(F_o^2)$	0.093	0.084
σ_1	1.71	1.64
no. of variables	252	441
data:param ratio	6.9:1	9.1:1

(20) Jones, S. B.; Petersen, J. L. *Inorg. Chem.* **1981**, *20*, 2889.

(21) Declerq, J. P.; Germain, D.; Main, P.; Woolfson, M. M. *Acta Crystallogr., Sect. A: Cryst. Phys., Diffr., Theor. Gen. Crystallogr.* **1973**, *A29*, 231.

(22) The least-squares refinement[23] of the X-ray diffraction data was based upon the minimization of $\sum w_i|F_o^2 - S^2F_c^2|^2$, where w_i is the individual weighting factor and S is the scale factor. The discrepancy indices were calculated from the expressions $R(F_o) = \sum||F_o| - |F_c||/\sum|F_o|$, $R(F_o^2) = \sum|F_o^2 - F_c^2|/\sum F_c^2$, and $R_w(F_o^2) = [\sum w_i|F_o^2 - F_c^2|^2/\sum w_i F_o^4]^{1/2}$. The standard deviation of an observation of unit weight, σ_1, equals $[\sum w_i|F_o^2 - F_c^2|/(n-p)]^{1/2}$, where n is the number of observations and p is the number of parameters varied during the last refinement cycle.

(23) The scattering factors employed in all of the structure factor calculations were those of Cromer and Mann[24] for the non-hydrogen atoms and those of Stewart et al.[25] for the hydrogen atoms with corrections included for anomalous dispersion.[26]

(24) Cromer, D. T.; Mann, J. B. *Acta Crystallogr., Sect. A: Cryst. Phys., Diffr., Theor. Gen. Crystallogr.* **1968**, *A24*, 321.

(25) Stewart, R. F.; Davidson, E. R.; Simpson, W. T. *J. Chem. Phys.* **1965**, *42*, 3175.

(26) Cromer, D. T.; Liberman, D. *J. Chem. Phys.* **1970**, *53*, 1891.

Table II. Positional Parameters for Non-Hydrogen Atoms in $(C_5H_5)_2Zr(N(CMe_3)C(CH_2SiMe_2CH_2)=CN(CMe_3))$[a]

atom	x	y	z
Zr	0.29890 (9)	0.75000	0.14339 (5)
Si	0.2062 (3)	0.5497 (4)	0.4333 (2)
N1	0.2362 (8)	0.8622 (10)	0.2516 (5)
N2	0.4526 (7)	0.6491 (9)	0.2490 (4)
C1	0.2413 (8)	0.7448 (18)	0.3043 (5)
C2	0.3506 (10)	0.6342 (10)	0.3039 (6)
C3	0.1213 (10)	0.7011 (10)	0.3576 (6)
C4	0.3286 (11)	0.4957 (12)	0.3551 (7)
C5	0.3092 (15)	0.6200 (19)	0.5432 (8)
C6	0.0690 (13)	0.4080 (13)	0.4509 (9)
C7	0.1590 (11)	0.9986 (11)	0.2764 (6)
C8	−0.0097 (12)	0.9814 (13)	0.2605 (8)
C9	0.2237 (14)	1.0347 (14)	0.3770 (8)
C10	0.1887 (14)	1.1273 (14)	0.2215 (9)
C11	0.5950 (10)	0.5631 (13)	0.2724 (6)
C12	0.5747 (12)	0.4025 (13)	0.2522 (8)
C13	0.6711 (11)	0.5983 (19)	0.3712 (7)
C14	0.7032 (11)	0.6138 (14)	0.2146 (8)
C15	0.4195 (18)	0.9950 (14)	0.1134 (10)
C16	0.5301 (14)	0.8875 (18)	0.1133 (9)
C17	0.4828 (17)	0.7988 (14)	0.0366 (10)
C18	0.3468 (18)	0.8516 (20)	−0.0079 (8)
C19	0.3032 (16)	0.9686 (19)	0.0409 (10)
C20	0.1003 (13)	0.5490 (16)	0.1453 (8)
C21	0.0240 (11)	0.6656 (15)	0.0984 (8)
C22	0.0764 (13)	0.6782 (15)	0.0161 (8)
C23	0.1816 (13)	0.5735 (16)	0.0142 (8)
C24	0.2001 (12)	0.4913 (12)	0.0944 (8)

[a] The estimated standard deviations for this and all subsequent tables refer to the least-significant figures.

Scheme I

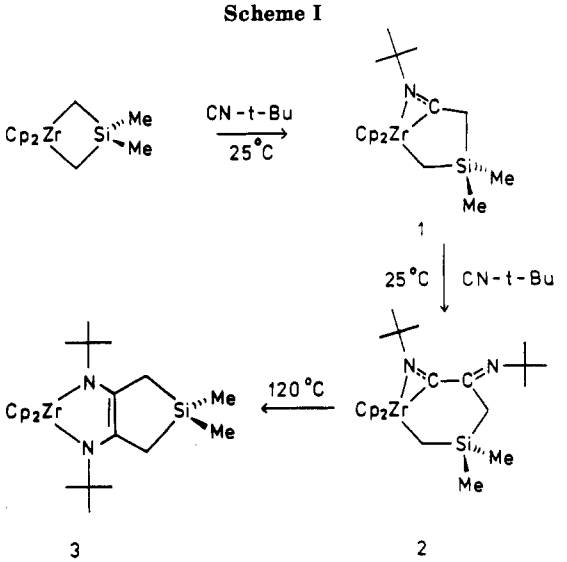

Results and Discussion

Reductive Coupling of CN-*t*-Bu by $Cp_2Zr(CH_2SiMe_2CH_2)$. The reaction scheme describing the sequence of chemical steps involved in the reductive coupling of two molecules of CN-*t*-Bu by $Cp_2Zr(CH_2SiMe_2CH_2)$ is depicted in Scheme I. Lateral insertion of the first equivalent of CN-*t*-Bu gives only $Cp_2Zr(N(CMe_3)CCH_2SiMe_2CH_2)$ (**1**).[16] This zirconadicyclic η^2-iminoacyl complex is thermodynamically stable at 25 °C and does *not* show any indication of undergoing an intramolecular 1,2-silyl shift rearrangement to the cyclic eneamide upon heating to 100 °C. The subsequent addition of 1 equiv of CN-*t*-Bu to 1 proceeds more slowly with the formation of a new C—C bond and affords the

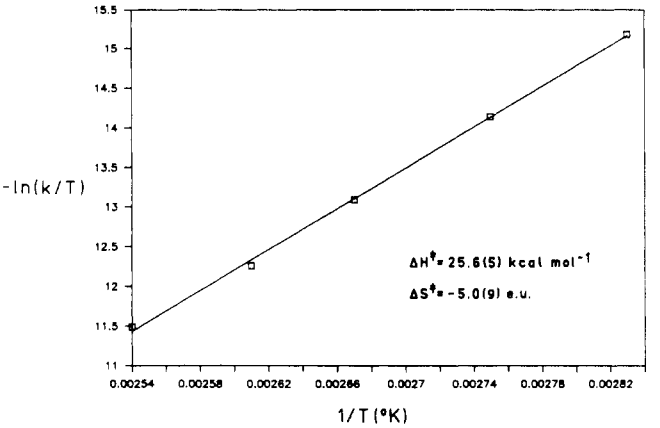

Figure 1. Eyring plot of $-\ln(k/T)$ vs $1/T$ for the intramolecular rearrangement of **2** to **3**.

Scheme II

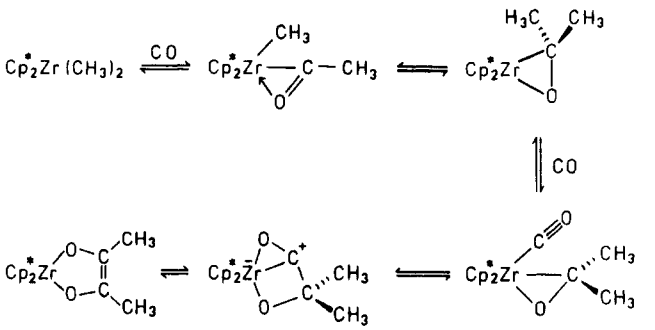

η^2-iminoacyl imine complex $Cp_2Zr(N(CMe_3)C—C(=NCMe_3)CH_2SiMe_2CH_2)$ (**2**).[16] Upon thermolysis, **2** rearranges solely to the bicyclic enediamidate $Cp_2Zr(N(CMe_3)C(CH_2SiMe_2CH_2)=CN(CMe_3))$ (**3**). The fact that the two methylene groups remain connected by $SiMe_2$ during the entire reaction sequence is consistent with the results of cross-over experiments that demonstrate the reductive coupling of CO by $Cp^*_2MMe_2$ (M = Th,[12] Zr[13]) occurs at a single metal center.

The reductive coupling process leading to the formation of **3** clearly involves three distinct steps. The first step in Scheme I is controlled by the ability of the electrophilic d^0 Zr(IV) center in $Cp_2Zr(CH_2SiMe_2CH_2)$ to mediate the initial insertion step and then stabilize the resultant η^2-iminoacyl fragment. The second phase relies on the electrophilic character of the "carbenium-like" carbon[27] of the η^2-iminoacyl group in **1** to provide a site for nucleophilic attack[28] by the second equivalent of CN-*t*-Bu. The final stage involves an unusual intramolecular rearrangement process, presumably initiated by a 1,2-migration of the Zr-bound methylene to the η^2-iminoacyl carbon atom of **2**. The activation parameters for the conversion of **2** to **3** were obtained by evaluating the temperature dependence of the rate constant, k. For the temperature range 80–120 °C, the corresponding rate constants are listed in Table VI. From the Eyring plot of $-\ln(k/T)$ vs $1/T$ shown in Figure 1, the activation parameters $\Delta H^‡ = 25.6$

(27) Tatsumi, K.; Nakamura, A.; Hofmann, P.; Stauffert, P.; Hoffmann, R. *J. Am. Chem. Soc.* **1985**, *107*, 4440.

(28) Related examples for η^2-acyl and η^2-silaacyl ligands include: (a) Labinger, J. A.; Bonfiglio, J. N.; Grimmett, D. L.; Masuo, S. T.; Shearin, E.; Miller, J. S. *Organometallics* **1983**, *2*, 733. (b) Karsch, H. H.; Müller, G.; Krüger, C. *J. Organomet. Chem.* **1985**, *273*, 195. (c) Bonnessen, P. V.; Yau, P. K. L.; Hersh, W. H. *Organometallics* **1987**, *6*, 1587. (d) Arnold, J.; Tilley, T. D.; Rheingold, A. L.; Geib, S. J.; Arif, A. T. *J. Am. Chem. Soc.* **1989**, *111*, 149 and references cited therein.

Table III. Positional Parameters for Atoms in $(C_5H_5)_2Zr(N(CMe_3)C(CH_2SiMe_2CH_2)=CN(xy))$

atom	x	y	z
Zr	0.16016 (2)	0.26003 (4)	0.87128 (1)
Si	0.46462 (7)	0.16370 (16)	0.84550 (5)
N1	0.2691 (2)	0.3367 (3)	0.9261 (1)
N2	0.2253 (2)	0.3210 (3)	0.7943 (1)
C1	0.3263 (2)	0.2908 (4)	0.8905 (2)
C2	0.3048 (2)	0.2709 (4)	0.8240 (2)
C3	0.4087 (3)	0.2069 (6)	0.9178 (2)
C4	0.3645 (2)	0.1761 (6)	0.7873 (2)
C5	0.5378 (4)	0.3348 (12)	0.8319 (4)
C6	0.5219 (6)	−0.0335 (11)	0.8486 (5)
C7	0.3017 (2)	0.4528 (5)	0.9875 (2)
C8	0.3369 (4)	0.3331 (7)	1.0409 (2)
C9	0.3670 (4)	0.5806 (7)	0.9735 (3)
C10	0.2281 (4)	0.5415 (8)	1.0121 (3)
C11	0.2180 (2)	0.3972 (4)	0.7324 (2)
C12	0.2513 (2)	0.5558 (4)	0.7284 (2)
C13	0.2372 (2)	0.6382 (5)	0.6700 (2)
C14	0.1923 (3)	0.5662 (5)	0.6166 (2)
C15	0.1616 (2)	0.4099 (5)	0.6204 (2)
C16	0.1744 (2)	0.3222 (5)	0.6780 (2)
C17	0.2993 (3)	0.6367 (6)	0.7861 (2)
C18	0.1431 (4)	0.1498 (6)	0.6798 (3)
C19	0.0880 (3)	0.5387 (5)	0.8753 (2)
C20	0.0689 (3)	0.4873 (6)	0.8138 (2)
C21	0.0176 (3)	0.3510 (7)	0.8138 (3)
C22	0.0031 (3)	0.3232 (6)	0.8768 (3)
C23	0.0493 (3)	0.4376 (6)	0.9153 (3)
C24	0.2251 (3)	−0.0332 (4)	0.8833 (2)
C25	0.1964 (3)	0.0038 (5)	0.9423 (2)
C26	0.1082 (3)	0.0111 (5)	0.9321 (2)
C27	0.0823 (3)	−0.0193 (5)	0.8672 (2)
C28	0.1534 (3)	−0.0445 (4)	0.8366 (2)
H1	0.442 (2)	0.270 (4)	0.950 (2)
H2	0.398 (2)	0.110 (5)	0.941 (2)
H3	0.345 (2)	0.082 (4)	0.779 (2)
H4	0.370 (2)	0.230 (4)	0.748 (2)
H5	0.552 (3)	0.327 (7)	0.794 (3)
H6	0.585 (4)	0.329 (7)	0.863 (3)
H7	0.511 (4)	0.428 (8)	0.838 (3)
H8	0.557 (4)	−0.033 (8)	0.874 (3)
H9	0.478 (3)	−0.118 (6)	0.864 (3)
H10	0.549 (4)	−0.055 (8)	0.812 (3)
H11	0.347 (2)	0.379 (5)	1.077 (2)
H12	0.296 (4)	0.236 (7)	1.050 (3)
H13	0.386 (3)	0.289 (6)	1.038 (2)
H14	0.339 (4)	0.669 (7)	0.943 (3)
H15	0.384 (3)	0.637 (6)	1.009 (2)
H16	0.414 (3)	0.532 (7)	0.955 (2)
H17	0.252 (3)	0.598 (5)	1.050 (2)
H18	0.185 (3)	0.473 (5)	1.018 (2)
H19	0.204 (3)	0.614 (5)	0.982 (2)
H20	0.258 (2)	0.751 (4)	0.671 (2)
H21	0.180 (2)	0.628 (5)	0.579 (2)
H22	0.129 (2)	0.352 (4)	0.583 (2)
H23	0.273 (3)	0.629 (5)	0.819 (2)
H24	0.313 (2)	0.757 (5)	0.778 (2)
H25	0.355 (3)	0.600 (5)	0.795 (2)
H26	0.117 (3)	0.121 (5)	0.643 (2)
H27	0.104 (3)	0.134 (5)	0.708 (2)
H28	0.195 (3)	0.068 (7)	0.694 (2)
H29	0.115 (2)	0.616 (5)	0.889 (2)
H30	0.089 (2)	0.530 (5)	0.781 (2)
H31	0.004 (3)	0.299 (6)	0.786 (2)
H32	−0.026 (3)	0.245 (5)	0.894 (2)
H33	0.053 (3)	0.449 (5)	0.958 (2)
H34	0.282 (2)	−0.051 (4)	0.879 (2)
H35	0.232 (2)	0.013 (5)	0.979 (2)
H36	0.076 (2)	0.035 (5)	0.965 (2)
H37	0.031 (2)	−0.019 (4)	0.850 (2)
H38	0.155 (2)	−0.070 (4)	0.794 (2)

(5) kcal mol^{-1} and $\Delta S^* = -5.0$ (9) eu were determined for this first-order process.

Our reaction scheme displays many of the same features as the one described recently by Roddick and Bercaw[14] to account for the reductive coupling reaction that occurs upon carbonylation of $Cp^*_2ZrMe_2$. As illustrated in Scheme II, the generation of $Cp^*_2Zr(OC(Me)=C(Me)O)$ involves two separate methyl migrations, one prior to and the other following the principal carbonyl-coupling step. Although the η^2-acetone adduct indicated in Scheme II has not been identified, Roddick and Bercaw have trapped an analogous hafnocene η^2-aldehyde intermediate with CO and have observed that $Cp^*_2Hf(\eta^2\text{-}OC(H)(CH_2CHMe_2))CO$ cleanly rearranges at 80 °C to the cyclic enediolate $Cp^*_2Hf(OC(CH_2CHMe_2)=C(H)O)$. Parallel MO calculations performed by Hofmann et al.[13] have further indicated that the CO ligand helps stabilize the zirconocene (η^2-acetone) intermediate proposed in Scheme II.

The corresponding reductive coupling step in Scheme I occurs much earlier in this reaction sequence. Apparently, migration of the zirconium-bound methylene to the electrophilic carbon of the η^2-iminoacyl group of **1** is disfavored, since it would form an intermediate containing a highly strained four-membered ring. However, following the conversion of **1** to **2**, the conditions for such an intramolecular 1,2-methylene shift may be more favorable because of the formation of a larger, less strained ring in the transition state. Subsequent rotation about the N–C(ring) bond of the resultant intermediate permits the lone pair of the exocyclic imine nitrogen to donate to the Zr. This interaction presumably sets into motion a series of bond

Table IV. Interatomic Distances (Å) and Bond Angles (deg) for the Non-Hydrogen Atoms in $(C_5H_5)_2Zr(N(CMe_3)C(CH_2SiMe_2CH_2)=CN(CMe_3))$[a,b]

A. Interatomic Distances

Zr–N1	2.111 (8)	Zr–N2	2.104 (6)
Zr–Cp(1)	2.285 (12)	Zr–Cp(2)	2.303 (9)
Zr–C1	2.564 (8)	Zr–C2	2.574 (9)
N1–C1	1.352 (17)	N2–C2	1.377 (12)
N1–C7	1.501 (14)	N1–C11	1.509 (12)
C1–C3	1.544 (13)	C2–C4	1.519 (14)
C3–Si	1.859 (9)	C4–Si	1.851 (12)
C5–Si	1.834 (13)	C6–Si	1.870 (13)
C7–C8	1.532 (15)	C11–C12	1.509 (17)
C7–C9	1.534 (14)	C11–C13	1.531 (14)
C7–C10	1.495 (17)	C11–C14	1.521 (16)
C1–C2	1.432 (16)		

range of Zr–C (Cp(1) ring): 2.530 (17)–2.596 (17)
range of Zr–C (Cp(2) ring): 2.576 (11)–2.605 (13)
range of C–C (Cp rings): 1.38 (2)–1.42 (2)

B. Bond Angles

N1–Zr–N2	84.1 (3)	Cp(1)–Zr–Cp(2)	121.2 (5)
Zr–N1–C1	93.0 (6)	Zr–N2–C2	93.0 (5)
Zr–N1–C7	144.8 (6)	Zr–N2–C11	145.3 (6)
C1–N1–C7	119.1 (8)	C2–N2–C11	118.6 (7)
N1–C1–C2	121.2 (8)	N2–C2–C1	120.0 (8)
N1–C1–C3	124.8 (9)	N2–C2–C4	124.1 (8)
C2–C1–C3	113.4 (11)	C1–C2–C4	115.2 (9)
C1–C3–Si	104.6 (7)	C2–C4–Si	104.7 (7)
C3–Si–C4	93.0 (5)	C5–Si–C6	111.1 (6)
C3–Si–C5	110.8 (6)	C4–Si–C5	112.8 (6)
C3–Si–C6	113.2 (5)	C4–Si–C6	114.8 (5)
N1–C7–C8	113.4 (8)	N2–C11–C12	113.5 (8)
N1–C7–C9	108.0 (8)	N2–C11–C13	108.4 (8)
N1–C7–C10	111.1 (9)	N2–C11–C14	110.4 (8)
C8–C7–C9	110.5 (10)	C12–C11–C13	114.4 (10)
C8–C7–C10	107.0 (9)	C12–C11–C14	104.8 (9)
C9–C7–C10	106.7 (9)	C13–C11–C14	104.9 (8)

range of C–C–C (Cp rings): 105.8 (11)–110.5 (12)

[a] Cp(n) denotes the centroid of a cyclopentadienyl ring. Cp(1) and Cp(2) include carbon atoms C15–C19 and C20–C24, respectively. [b] The esd's for the interatomic distances and bond angles were calculated from the standard errors for the fractional coordinates of the corresponding atomic positions.

Table V. Interatomic Distances (Å) and Bond Angles (deg) for the Non-Hydrogen Atoms in $(C_5H_5)_2Zr(N(CMe_3)C(CH_2SiMe_2CH_2)=CN(xy))$[a,b]

A. Interatomic Distances

Zr–N1	2.127 (3)	Zr–N2	2.080 (3)
Zr–Cp(1)	2.258 (5)	Zr–Cp(2)	2.306 (4)
Zr–C1	2.612 (3)	Zr–C2	2.603 (3)
N1–C1	1.387 (4)	N2–C2	1.389 (4)
N1–C7	1.498 (4)	N2–C11	1.428 (4)
C1–C3	1.516 (5)	C2–C4	1.503 (5)
C3–Si	1.880 (4)	C4–Si	1.869 (4)
C5–Si	1.858 (9)	C6–Si	1.844 (9)
C1–C2	1.398 (5)	C7–C8	1.534 (6)
C7–C9	1.522 (7)	C7–C10	1.513 (8)
C12–C17	1.494 (6)	C16–C18	1.494 (7)

range of Zr–C (Cp(1) ring): 2.523 (5)–2.553 (5)
range of Zr–C (Cp(2) ring): 2.588 (4)–2.605 (4)
range of C–C (Cp rings): 1.349 (7)–1.400 (6)
range of C–C (xy ring): 1.372 (6)–1.404 (5)

B. Bond Angles

N1–Zr–N2	82.7 (1)	Cp(1)–Zr–Cp(2)	123.9 (2)
Zr–N1–C1	93.7 (2)	Zr–N2–C2	95.2 (2)
Zr–N1–C7	145.0 (2)	Zr–N2–C11	144.8 (2)
C1–N1–C7	119.7 (3)	C2–N2–C11	119.8 (3)
N1–C1–C2	119.7 (3)	N2–C2–C1	120.1 (3)
N1–C1–C3	125.8 (3)	N2–C2–C4	120.8 (3)
C2–C1–C3	114.2 (3)	C1–C2–C4	118.7 (3)
C1–C3–Si	104.5 (3)	C2–C4–Si	103.2 (3)
C3–Si–C4	94.0 (2)	C5–Si–C6	110.6 (4)
C3–Si–C5	110.3 (3)	C4–Si–C5	110.4 (3)
C3–Si–C6	114.4 (3)	C4–Si–C6	116.1 (3)
N1–C7–C8	112.3 (3)	C8–C7–C9	112.7 (4)
N1–C7–C9	108.8 (3)	C8–C7–C10	106.2 (4)
N1–C7–C10	108.9 (3)	C9–C7–C10	107.8 (4)
N2–C11–C12	117.9 (3)	N2–C11–C16	121.5 (3)

range of C–C–C (Cp rings): 107.0 (5)–109.4 (4)
range of C–C–C (xy ring): 118.7 (3)–121.5 (3)

[a] Cp(n) denotes the centroid of a cyclopentadienyl ring. Cp(1) and Cp(2) contain carbon atoms C19–C23 and C24–C28, respectively. [b] The esd's for the interatomic distances and bond angles were calculated from the standard errors for the fractional coordinates of the corresponding atomic positions.

Table VI. Rate Constants for the Intramolecular Rearrangement of 2 → 3

T, °C	k, s^{-1}	$t_{1/2}$, min
80.0	$9.0\ (3) \times 10^{-5}$	128
90.0	$2.62\ (6) \times 10^{-4}$	44
100.7	$7.7\ (2) \times 10^{-4}$	15
110.0	$1.82\ (5) \times 10^{-3}$	6.3
120.0	$4.01\ (10) \times 10^{-3}$	2.9

reorganization steps involved in the construction of the second five-membered ring of the chelating enediamido ligand of **3**. The presence of the 1-sila-3-zirconacyclobutane ring in $Cp_2Zr(CH_2SiMe_2CH_2)$ clearly affects the sequence of chemical events involved in the reductive coupling process.[29]

Characterization of $Cp_2Zr(N(CMe_3)C(CH_2SiMe_2CH_2)=CN(CMe_3))$ (3). Of the three zirconacyclic species in Scheme I, only the characterization of **3** has not been described previously.[16] The identity of **3** has been confirmed by a combination of spectroscopic and structural methods of analysis (vide infra). The ^1H and ^{13}C NMR data indicate that the ZrN_2C_2 ring is folded significantly along the N···N vector. The inequivalence of the two cyclopentadienyl rings and the two methyl groups of $SiMe_2$ in **3** leads to the observation of two distinct resonances in both the ^1H and $^{13}C\{^1H\}$ NMR spectra for the Cp rings and for the methyl groups. In addition, the methylene protons give an AB quartet at δ 2.01 and 1.20 with a geminal coupling constant of 16.9 Hz. The corresponding methylene carbon resonance, however, in the gated nondecoupled ^{13}C NMR spectrum appears as a "pseudo" triplet at δ 22.4, thus indicating that $^1J_{^{13}C-H_A}$ and $^1J_{^{13}C-H_B}$ are essentially equal.

Further spectroscopic evidence of the nonplanarity of the ZrN_2C_2 ring in **3** is provided by the location of the electronic absorption band, corresponding to electron excitation from the filled π-orbital of the C=C bond to an empty d_{z^2}-like orbital on the zirconium. Hofmann and co-workers[3] observed in related cyclic enediolate complexes, $Cp^*_2Zr(OC(R)=C(R)O)$, where R = Me, CMe_3, that this band shifts to lower wavelength as the folding of the ZrO_2C_2 ring along the O···O vector increases. A similar spectral trend is observed for $Cp^*_2Zr(N(Me)C(CH_2SiMe_2CH_2)=CN(Me))$ and **3**. Although the solution ^1H and ^{13}C NMR spectra[16] of $Cp^*_2Zr(N(Me)C(CH_2SiMe_2CH_2)=CN(Me))$ at 25 °C are compatible with a planar bicyclic ring structure, its ZrN_2C_2 ring is folded by 35.7° in the solid state.[30] Whereas λ_{max} for this dark blue complex is 546 nm, λ_{max} for **3** is 352 nm. The magnitude of the shift observed for this electronic absorption band indicates that the ZrN_2C_2 of **3** should be folded to a much greater extent (vide infra).

Mechanistic Considerations. An important aspect of Scheme I is the site of attack by the second molecule of CN-*t*-Bu. By virtue of the steric bulk of the *tert*-butyl group in **1** and the electrophilic character of its η^2-iminoacyl carbon, nucleophilic addition presumably occurs at this carbenium-like center. In an attempt to monitor the course of the subsequent insertion reaction leading to the formation of **2**, the reaction of **1** with 2,6-xylyl isocyanide was performed. In this case, the initial species formed upon nucleophilic attack of CN(xy) at the η^2-iminoacyl carbon of **1** could rearrange to give two possible isomers: $Cp_2Zr(N(CMe_3)C—C(=N(xy))CH_2SiMe_2CH_2)$ (**4a**) and $Cp_2Zr(N(xy)C—C(=NCMe_3)CH_2SiMe_2CH_2)$ (**4b**). The formation of **4a** presumably proceeds with retention of the η^2-iminoacyl—Zr interaction of **1** and involves the occurrence of an intramolecular 1,2-methylene shift. In contrast, the formation of **4b** requires the displacement of the original η^2-iminoacyl group from the Zr and does not necessitate the breaking of the C(η^2-iminoacyl)—C(methylene) bond of **1**. Unfortunately, this reaction (1) proceeds

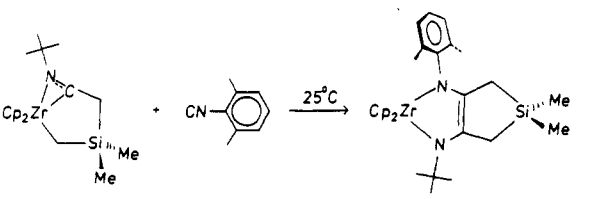

(1)

1 5

directly at 25 °C with reductive coupling to the bicyclic enediamidate $Cp_2Zr(N(CMe_3)C(CH_2SiMe_2CH_2)=CN-$

(29) A similar reaction sequence may be operative for the coupling of 2,6-xylyl isocyanide by Cp*Ti(2,3-dimethyl-1,3-butadiene)Cl. See: Hessen, B.; Blenkers, J.; Teuben, J. H.; Helgesson, G.; Jagner, S. *Organometallics* **1989**, *8*, 830.

(30) Berg, F. J.; Petersen, J. L., work in progress.

Scheme III

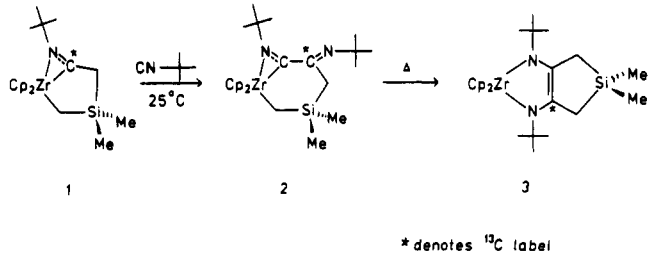

(xy)) (5). Although the appearance during a separate NMR tube experiment of an upfield methylene proton resonance at δ −0.14 provides evidence of the formation of an intermediate η^2-iminoacyl imine complex, attempts to isolate this species for purposes of determining the location of the 2,6-xylyl substituent have not been successful.

The identity of 5 has been confirmed by spectroscopic and crystallographic methods (vide infra). The spectral features observed in the NMR and electronic spectra of 5 are analogous to those displayed by 3. However, the presence of the 2,6-xylyl group in 5 further complicates the NMR spectra by eliminating the mirror plane of symmetry possessed by 3. The two pairs of methylene protons in 5 are not chemically equivalent, and therefore each appears as a separate AB quartet. One doublet of doublets is located at δ 2.09, 1.55 with $^1J_{H-H}$ = 17.0 Hz, while the other one is located at δ 1.29, 1.06 with $^1J_{H-H}$ = 17.8 Hz. The corresponding methylene carbon resonances in the gated nondecoupled ^{13}C NMR spectrum appear as separate "pseudo" triplets at δ 22.1 and 16.9. The absorption band for the $\pi(C{=}C) \rightarrow d_{z^2}(Zr)$ transition in 5 occurs at λ_{max} = 366 nm, indicating that the degree of folding of the ZrN_2C_2 ring in 5 is comparable to that in 3.

As an alternative approach for investigating the insertion pathway leading to the formation of 2, a ^{13}C-enriched sample of 1 was prepared by reacting equimolar amounts of $Cp_2Zr(CH_2SiMe_2CH_2)$ and ca. 20% ^{13}C-enriched ^{13}CN-*t*-Bu and then treated with a second equivalent of naturally abundant CN-*t*-Bu in a sealed NMR tube. Periodic $^{13}C\{^1H\}$ NMR measurements indicate that the reaction proceeds at 25 °C with only the intensity of the imine carbon resonance of 2 at δ 169.3 being enhanced. From this observation, the second insertion step in Scheme I does *not* involve a 1,2-methylene shift (as we previously suggested[16]) but proceeds via displacement of the original η^2-iminoacyl group of 1 upon coordination of the isonitrile. After this sample was heated at 120 °C for 20 min, ^{13}C NMR measurements revealed that the thermally induced rearrangement of 2 to 3 is accompanied by the expected enhancement of the product's ^{13}C NMR resonance at δ 122.3 (Scheme III).

Although the deinsertion of CN-*t*-Bu during this rearrangement seems remote, the reaction of 2 with an equivalent amount of 2,6-xylyl isocyanide was performed to evaluate this possibility. If deinsertion occurs to any appreciable extent, then the reaction should yield a mixture of 3 and 5. Following the heating of an NMR tube containing these reactants at 60 °C for several days, $^{13}C\{^1H\}$ NMR measurements showed only the presence of 3 and no evidence for the formation of 5 within NMR detection limits. These experimental results thereby rule out the possible importance of such a deinsertion step during the intramolecular rearrangement of 2 to 3.

Description of the Molecular Structures of $Cp_2Zr(N(CMe_3)C(CH_2SiMe_2CH_2)=CN(R))$, R = CMe_3 (3), 2,6-Xylyl (5). The crystal structures of 3 and 5 have been determined by X-ray diffraction methods. The former compound crystallizes in the noncentrosymmetric monoclinic space group $P2_1$, whereas the latter compound crystallizes in the centrosymmetric monoclinic space group $P2_1/c$. Perspective views of the molecular structures of 3 and 5 are illustrated in Figures 2 and 3, respectively, with appropriate atom-labeling schemes.

The pseudotetrahedral ligand environment about the Zr atom in 3 and 5 consists of two π-bonded cyclopentadienyl rings and the N-donors of the enediamido ligand. The five-membered ZrN_2C_2 ring is folded along the N1···N2 vector with the dihedral angle between the planes containing atoms Zr, N1, and N2 and atoms N1, N2, C1, and C2 being 52.1 and 51.3° in 3 and 5, respectively. As a result, carbon atoms C1 and C2 are displaced

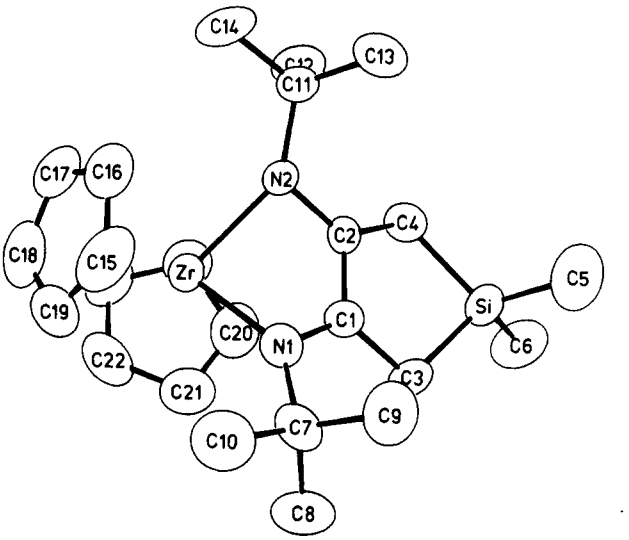

Figure 2. Perspective view of the molecular structure of $Cp_2Zr(N(CMe_3)C(CH_2SiMe_2CH_2)=CN(CMe_3))$ (3) with the atom-numbering scheme. The thermal ellipsoids are scaled to 50% probability. The hydrogen atoms have been omitted for clarity.

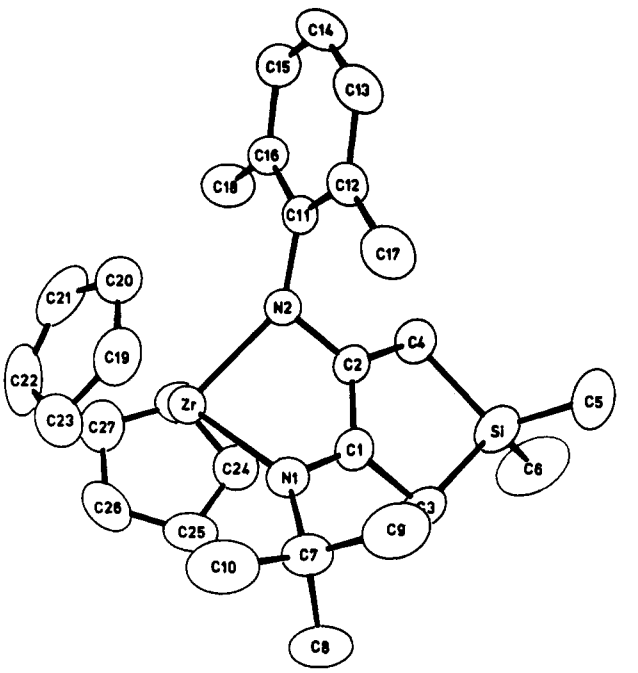

Figure 3. Perspective view of the molecular structure of $Cp_2Zr(N(CMe_3)C(CH_2SiMe_2CH_2)=CN(xy))$ (5) with the atom-labeling scheme. The thermal ellipsoids are scaled to 50% probability. The hydrogen atoms have been omitted.

by 0.92–0.95 Å from the Zr, N1, N2 plane that bisects the dihedral angle between the planar cyclopentadienyl rings. The nonplanarity of the ZrN_2C_2 ring is compatible with the structures reported for numerous other group 4 complexes containing a chelating eneamidolato,[5c] enediamido,[5b,5c,8] or *cis*(butadiene)[31] ligand. An important consequence of the folding of this five-membered ring is the π-bonding interaction brought about by moving the two carbon atoms of the ZrN_2C_2 ring closer to the electron-deficient metal center. The Zr–Cl and Zr–C2 distances of 2.564 (8) and 2.574 (9) Å in **3** and 2.612 (3) and 2.603 (3) Å in **5**, respectively, are comparable to the corresponding zirconium–cyclopentadienyl ring carbon distances that range from 2.52 to 2.61 Å in these two compounds. Rothwell et al.[5c] have reported that extended Hückel MO calculations carried out by Tatsumi and coworkers on $(MeO)_2Zr(N(Me)C(Me)=C(Me)N(Me))$ show a small attractive interaction between the electron-deficient Zr(IV) center and the carbons of the NC=CN unit.

The coordination environment about the Zr atom in **3** and **5** is quite crowded. The Cp(1)–Zr–Cp(2) angles of 121.2 (5) and 123.9 (2)° in **3** and **5**, respectively, reflect a significant increase in the canting of each pair of cyclopentadienyl rings. The bending of the ZrN_2C_2 ring further helps to relieve the steric interactions between the cyclopentadienyl rings and the *tert*-butyl and 2,6-xylyl substituents of the enediamido ligands. In spite of the steric congestion about the Zr atom, the short Zr–N distances indicate a considerable degree of pπ donation from N1 and N2 to the metal. A notable result of this pπ–dπ interaction is the concomitant increase in the average Zr–C(Cp) bond distance, which is 0.07 Å longer than in $Cp_2Zr(CH_2SiMe_2CH_2)$.[32]

The coordination mode of the chelating enediamido ligand can be viewed as either a neutral α-diimine interacting with a d^2 Zr(II) center (resonance structure A) or

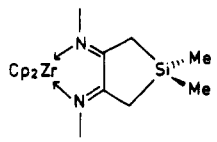

A

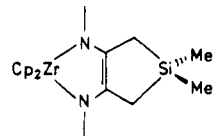

B

a dianionic enediamido ligand donating to a d^0 Zr(IV) center (resonance structure B). The structural parameters within the 1,4-diaza-5-zirconacyclopentene ring of **3** and of **5** are consistent with this latter bonding description. The C–N distances of 1.352 (17) and 1.377 (12) Å in **3** and 1.387 (4) and 1.389 (4) Å in **5** are significantly longer than the C=N distance of 1.257 (2) Å in the uncoordinated 1,4-diaza-1,3-butadiene compound, $C_6H_{11}N=CHCH=N-C_6H_{11}$.[33] The C1—C2 bond distances of 1.432 (16) Å in **3** and 1.398 (5) Å in **5** are significantly shorter than a normal C—C single bond and are comparable to the range 1.35–1.42 Å observed for the corresponding bonds in related eneamidolate,[5c] enediamidate,[5b,5c,8] and butadiene[31] complexes that adopt the metallacyclopentene resonance form. Finally, the Zr—N distances of 2.11 ± 0.02 Å in **3** and **5** are consistent with the Zr—N bond distances reported for π-donating dialkylamido groups bound to Zr(IV).[34] The noticeably shorter Zr—N2 distance of 2.080 (3) Å in **5** is presumably a consequence of the resonance stabilization introduced by the 2,6-xylyl substituent.

Dynamic Behavior of $Cp_2Zr(N(CMe_3)C(CH_2SiMe_2CH_2)=CN(R))$, R = CMe_3 (3), 2,6-Xylyl (5). An interesting feature normally associated with group 4 metal complexes containing a nonplanar, five-membered ring is their dynamic behavior in solution. For an σ^2,π-coordinated enediamido ligand, this fluxionality is associated with the interconversion between the two folded conformations of the 1,4-diaza-5-metallacyclopentene ring. From the coalescence temperature of the nonequivalent aryl oxide and xylyl methyl resonances in the ^1H NMR spectrum of $Zr(OAr')_2(NC(xy)C(Me)=C(Me)N(xy))$, where OAr' = 2,6-di-*tert*-butylphenoxide, Rothwell and coworkers[5b] estimated an inversion barrier of 14.5 (5) kcal/mol at 0 °C for this degenerate rearrangement process. In contrast, the nonplanarity of the ZrN_2C_2 ring of **3** and **5** makes the proton resonances of the two methyl groups of $SiMe_2$, of the methylene protons, and of the cyclopentadienyl rings inequivalent at room temperature. Upon heating in toluene-d_8[35] to 150 °C, three distinct exchange processes are observed for **3**, whereas the corresponding resonances in the ^1H NMR spectrum of **5** remain essentially unchanged. From the corresponding rate constant[36] at each coalescence temperature (T_c), the free energy barrier ΔG^* has been estimated as 16.7 (5) kcal/mol (52 ± 1 °C) for the methyl groups, 18.4 (5) kcal/mol (120 ± 1 °C) for the methylene protons, and 19.5 (5) kcal/mol (142 ± 1 °C) for the cyclopentadienyl ring protons. These data clearly indicate that the inversion of the bicyclic enediamidate ligand in **3** occurs in stages, with the final flipping of the ZrN_2C_2 ring having the highest activation barrier. This relatively large inversion barrier of ca. 20 kcal/mol for **3** probably stems from the greater steric congestion at zirconium. In addition, it is apparent that the dynamic behavior of these enediamido complexes is significantly influenced by the nitrogen substituents.

Concluding Remarks. Our investigations of the reductive coupling of CN-*t*-Bu with $Cp_2Zr(CH_2SiMe_2CH_2)$ have allowed us to isolate two η^2-iminoacyl–Zr intermediates, **1** and **2**, that participate in the formation of the enediamido product **3** and to observe an unusual intramolecular rearrangement during the thermally induced conversion of **2** to **3**. The major chemical steps of this reaction sequence (Scheme I) are comparable to those proposed for the reductive coupling of CO by $Cp^*_2ZrMe_2$. The primary difference is that the C–C-bond-forming step occurs much earlier during the reductive coupling of CN-*t*-Bu by $Cp_2Zr(CH_2SiMe_2CH_2)$. The alternative chronology of chemical events in Scheme I reflects the greater preference of the η^2-iminoacyl carbon of **1** to attack by an external nucleophile (i.e., CN-*t*-Bu) than to intramolecular

(31) (a) Erker, G.; Engel, K.; Krüger, C.; Muller, G. *Organometallics* **1984**, *3*, 128. (b) Erker, G.; Krüger, C.; Muller, G. *Adv. Organomet. Chem.* **1985**, *24*, 1 and references cited therein.
(32) Tikkanen, W. R.; Egan, J. W., Jr.; Petersen, J. L. *Organometallics* **1984**, *3*, 1646.
(33) Van Koten, G.; Vrieze, A. *Adv. Organomet. Chem.* **1982**, *21*, 153.
(34) Lappert, M. F.; Sanger, A. R.; Srivastava, R. C.; Power, P. P. *Metal and Metalloid Amides*; Horwood-Wiley: New York, 1979.
(35) Slow-exchange ^1H NMR spectrum (−75 °C) of **3** (toluene-d_8): 6.07, 5.33 (C_5H_5, s), 2.02, 1.16 (CH_aH_b, d, 16.9 Hz), 1.40 ($NCCH_3$, s), 0.26, 0.19 ($SiCH_3$, s).
(36) For the uncoupled pair of singlets corresponding to the proton resonances of the methyl groups and of the cyclopentadienyl rings, the rate constant at the coalescence temperature was calculated from $k_c = 2.22(\Delta\nu_{AB})$.[37] For the coupled methylene protons, k_c was calculated from $k_c = 2.22(\Delta\nu_{AB}^2 + 6J_{AB}^2)^{1/2}$, where $\Delta\nu_{AB}$ is the difference in the corresponding proton frequencies in the slow-exchange limit.[38] The free energy of activation was calculated from the expression $\Delta G^* = 4.576T_c(10.319 + \log T_c - \log k_c)$.
(37) Gutowsky, H. S.; Holm, C. H. *J. Chem. Phys.* **1956**, *25*, 1228.
(38) Kurland, R. J.; Rubin, M. B.; Wise, W. B. *J. Chem. Phys.* **1964**, *40*, 2426.

migration of its Zr-bound methylene group. The increased ring strain that would be introduced by such a 1,2-methylene shift apparently provides a sufficient activation barrier to preclude its occurrence. Molecular orbital calculations on **1** and **2** will be undertaken to evaluate the orbital character of the LUMO in these complexes. Their outcome may provide further insight into the role of the respective η^2-iminoacyl carbon centers in the overall reductive coupling process.

Acknowledgment. Support for this research was provided by the donors of the Petroleum Research Fund, administered by the American Chemical Society. J.L.P. further expresses his appreciation to Dr. P. Fagan and Professors W. R. Moore and A. Stolzenberg for helpful suggestions. Computer time for the X-ray structural analyses was provided by the West Virginia Network for Educational Telecomputing.

Supplementary Material Available: Tables of thermal parameters, pertinent least-squares planes for **3** and **5**, and the atomic coordinates for the hydrogen atoms of **3** (12 pages); listings of observed and calculated structure factors for **3** and **5** (19 pages). Ordering information is given on any current masthead page.

In-Plane Olefin Coordination and Unusually Small Substituent Dependency of Stability in (η^3-Allyl)(pentafluorophenyl)(olefin)-platinum(II) Complexes

Hideo Kurosawa,* Kunio Miki,† Nobutami Kasai,* and Isao Ikeda

Department of Applied Chemistry, Faculty of Engineering, Osaka University, Suita, Osaka 565, Japan

Received September 7, 1990

The crystal structure of the styrene complex Pt(η^3-CH_2CMeCH_2)(CH_2=CHC_6H_5)(C_6F_5) (**2a**) was determined. Crystal data: $C_{18}H_{15}F_5Pt$, fw = 521.40, triclinic, space group $P\bar{1}$, a = 6.292 (2) Å, b = 11.874 (4) Å, c = 12.736 (4) Å, α = 117.39 (2)°, β = 82.07 (3)°, γ = 97.50 (4)°, V = 834.3 (5) Å^3, Z = 2, D_c = 2.075 g cm^{-3}, R = 0.074 for 3410 reflections ($|F_o| > 3\sigma(|F_o|)$). The structure thus determined revealed the C=C bond of styrene oriented parallel to the coordination plane (the angle between the C=C axis and the coordination plane is 10.2°). When dissolved in $CDCl_3$, **2a** takes two isomeric forms. The ^{1}H NMR NOE experiments indicated that the configuration of the major isomer in solution is similar to that in the solid state. The minor isomer corresponds to a diastereomer of the major isomer, where both isomers contain the C=C bond lying almost in the coordination plane. The measurements of the epimerization rate of **2a** in the absence and presence of free styrene suggested that the interconversion between the two isomers is an intramolecular process without invoking Pt–styrene bond dissociation. Substituted styrene complexes Pt(η^3-CH_2CMeCH_2)(CH_2=CHC_6H_4Y)(C_6F_5) (**2b–f**) (Y = *m*-NO_2, *p*-Cl, *p*-Me, *p*-OMe, *o*-Me) were generated by ligand exchange between **2a** and appropriate olefin. Relative olefin coordination ability was determined by ^{1}H NMR analysis of an equilibrium mixture containing **2a**, a substituted styrene complex, **2b–f**, and the appropriate olefins to show the stability trend unusually weakly dependent on the electronic property of the substituent Y (Hammett ρ = −0.38). The nature of the Pt–olefin bond in **2** has been discussed in terms of these stability and structural trends.

Olefin complexes of transition metals simultaneously containing η^3-allyl ligands have received increasing attention from both coordination[1] and synthetic[2] chemical points of view. The studies on the cationic olefin complexes of the type [Pt(η^3-CH_2CMeCH_2)(olefin)(PPh_3)]$^+$ (**1**)

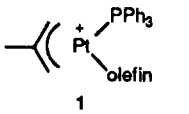

1

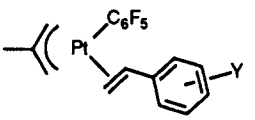

2a, Y = H
b, Y = *m*-NO_2
c, Y = *p*-Cl
d, Y = *p*-Me
e, Y = *p*-OMe
f, Y = *o*-Me

have revealed[1b] that these are somewhat unique in terms of the nature of metal–olefin bond when compared to the classic, more ordinary olefin complexes of Pt(II) such as Zeise's salt. That is, the former class complexes contain the C=C bond oriented parallel to the coordination plane (in-plane geometry)[1b,c,e] if the steric effect is not significant, in contrast to that oriented perpendicular (upright geometry) in the latter class.[3] This difference was brought about primarily by the different steric requirement around

† Present address: Research Laboratory of Resources Utilization, Tokyo Institute of Technology, Nagatsuda, Yokohama 227, Japan.

(1) (a) Grassi, M.; Meille, S. V.; Musco, A.; Pontellini, R.; Sironi, A. *J. Chem. Soc., Dalton Trans.* **1990**, 251–255. (b) Miki, K.; Yamatoya, K.; Kasai, N.; Kurosawa, H.; Urabe, A.; Emoto, M.; Tatsumi, K.; Nakamura, A. *J. Am. Chem. Soc.* **1988**, *110*, 3191–3198. (c) Musco, A.; Pontellini, R.; Grassi, M.; Sironi, A.; Meille, S. V.; Ruegger, H.; Ammann, C.; Pregosin, P. S. *Organometallics* **1988**, *7*, 2130–2137. (d) Ciajolo, R.; Jama, M. A.; Tuzi, A.; Vitagliano, A. *J. Organomet. Chem.* **1985**, *295*, 233–238. (e) Miki, K.; Kai, Y.; Kasai, N.; Kurosawa, H. *J. Am. Chem. Soc.* **1983**, *105*, 2482–2483. (f) Kurosawa, H.; Asada, N. *Organometallics* **1983**, *2*, 251–257. (g) Kurosawa, H.; Asada, N. *J. Organomet. Chem.* **1981**, *217*, 259–266.

(2) (a) Kurosawa, H.; Ogoshi, S.; Kawasaki, Y.; Murai, S.; Miyoshi, M.; Ikeda, I. *J. Am. Chem. Soc.* **1990**, *112*, 2813–2814. (b) Negishi, E.; Iyer, S.; Rousset, C. J. *Tetrahedron Lett.* **1989**, *30*, 291–294. (c) Oppolzer, W.; Bedoya-Zurita, M.; Switzer, C. Y. *Ibid.* **1988**, *29*, 6433–6436. (d) Kurosawa, H.; Emoto, M.; Ohnishi, H.; Miki, K.; Kasai, N.; Tatsumi, K.; Nakamura, A. *J. Am. Chem. Soc.* **1987**, *109*, 6333–6340. (e) Goliaszewski, A.; Schwartz, J. *Tetrahedron* **1985**, *41*, 5779–5789 and references therein. (f) Hosokawa, T.; Uno, T.; Inui, S.; Murahashi, S. *J. Am. Chem. Soc.* **1981**, *103*, 2318–2323.

(3) Ittel, S.; Ibers, J. A. *Adv. Organomet. Chem.* **1976**, *14*, 33.

0276-7333/91/2310-1607$02.50/0